Characterisation of the natural attenuation of chromium contamination in the presence of nitrate using isotopic methods. A case study from the Matanza-Riachuelo river basin, Argentina.

Elina Ceballos, Rosanna Margalef-Martí, Raul Carrey, Robert Frei, Neus Otero, Albert Soler, Carlos Ayora

Science of the total Environment, 2020, Volume 699, 134331
DOI: https://doi.org/10.1016/j.scitotenv.2019.134331

Received date: 27 May 2019
Revised date: 10 August 2019
Accepted date: 5 September 2019
Available online: 9 September 2019

CHARACTERISATION OF THE NATURAL ATTENUATION OF CHROMIUM CONTAMINATION IN THE PRESENCE OF NITRATE USING ISOTOPIC METHODS. A CASE STUDY FROM THE MATANZA-RIACHUELO RIVER BASIN, ARGENTINA

Elina Ceballos[a], Rosanna Margalef-Martí [b], Raul Carrey[b], Robert Frei[c], Neus Otero[b,d], Albert Soler[b], Carlos Ayora[e]

[a] Instituto de Hidrología de Llanuras "Dr. Eduardo J. Usunoff", CONICET-UNCPBA-CiC, República de Italia 780, 47 (B7300), Azul, Buenos Aires, Argentina

[b]Grup MAiMA, SGR Mineralogia Aplicada, Geoquímica i Geomicrobiologia, Departament de Mineralogia, Petrologia i Geologia Aplicada, Facultat de Ciències de la Terra, Universitat de Barcelona, UB, C/Martí i Franquès, s/n, 08028 Barcelona, Spain

[c]Department of Geosciences and Natural Resource Management, University of Copenhagen, Copenhagen, Denmark

[d]Serra Húnter Fellow, Generalitat de Catalunya, Spain

[e]Departament of Geoscience, Institute of Environmental Assessment and Water Research, IDAEA-CSIC, C/Jordi Girona, 18, 08028 Barcelona, Spain

eceballos@faa.unicen.edu.ar

Abstract

The groundwater contamination by hexavalent chromium (Cr(VI)) in a site of the Matanza-Riachuelo river basin (MRB), Argentina, has been evaluated by determining the processes that control the natural mobility and attenuation of

Cr(VI) in the presence of high nitrate (NO_3^-) contents. The groundwater Cr(VI) concentrations ranged between 1.9E-5 mM and 0.04 mM, while the NO_3^- concentrations ranged between 0.5 mM and 3.9 mM.

In order to evaluate the natural attenuation of Cr(VI) and NO_3^- in the MRB groundwater, Cr and N isotopes were measured in these contaminants. In addition, laboratory batch experiments were performed to determine the isotope fractionation (ε) during the reduction of Cr(VI) under denitrifying conditions. While the Cr(VI) reduction rate is not affected by the presence of NO_3^-, the NO_3^- attenuation is slower in the presence of Cr(VI). Nevertheless, no significant differences on ε values were observed when testing the absence or presence of each contaminant. The $\varepsilon^{53}Cr$ determined in the batch experiments describe a two- stage trend, in which Stage I is characterized by $\varepsilon^{53}Cr \sim -1.8$ ‰ and Stage II by $\varepsilon^{53}Cr \sim -0.9$ ‰. The respective $\varepsilon^{15}N_{NO3}$ obtained is -23.9 ‰ whereas $\varepsilon^{18}O_{NO3}$ amount to -25.7 ‰. Using these ε values and a Rayleigh fractionation model we estimate that an average of 60% of the original Cr(VI) is removed from the groundwater of the contaminated site. Moreover, the average degree of NO_3^- attenuation by denitrification is found to be about 20%. This study provides valuable information about the dynamics of a complex system that can serve as a basis for efficient management of contaminated groundwater in the most populated and industrialized basin of Argentina.

Keywords: Cr(VI) reduction, denitrification, isotopic fractionation, groundwater, Matanza-Riachuelo basin

1. INTRODUCTION

Chromium (Cr) is a toxic contaminant in groundwater derived mostly from anthropogenic activities such as metallurgic, refractory, chemical, and tannery industries. In aquatic environments, Cr exists in two main oxidation states, Cr(VI) and Cr(III). Cr(VI) is more toxic and generally more mobile than Cr(III). The oxidized form, Cr(VI), can cause cancer and dermatitis (Kotas and Stasicka, 2000). In contrast, the reduced form, Cr(III), is an essential nutrient, it is less soluble, adsorbs strongly on solid surfaces and co-precipitates with Fe(III) hydroxides (Rai et al., 1987; Davis and Olsen, 1995). Furthermore, Cr(VI) can be naturally reduced through biotic or abiotic oxidation of electron donors such as aqueous Fe(II), Fe(II)-bearing minerals, reduced sulfur species and organic compounds (Palmer and Wittbrodt, 1991). Reduction of toxic Cr(VI) to less toxic Cr(III) is an important process for attenuating Cr(VI) contamination in groundwater by immobilization as Cr(III) (Palmer and Puls, 1994; Davis and Olsen, 1995). This natural process can be enhanced or induced by adding an external electron donor to promote biotic and/or abiotic reduction (Blowes et al., 2000; Mayer et al., 2001b; Ellis et al., 2002; Wilkin et al., 2005; Wanner et al., 2012c; Jamieson-Hanes et al., 2012; Han et al., 2012; Basu et al., 2014).

Nitrate (NO_3^-) is another contaminant commonly found in groundwater (Rivett et al, 2008). Nitrate can also be reduced to N_2 gas through biotic or abiotic reactions (Korom, 1992). Denitrification is the main natural process to attenuate NO_3^- contamination in groundwater. Denitrification occurs under anaerobic conditions or dissolved oxygen concentrations below 2 mg/L (Korom, 1992; Cey et al., 1999). This process irreversibly eliminates NO_3^- from groundwater by reduction to N_2 through several intermediate steps ($NO_3^- \rightarrow NO_2^- \rightarrow NO \rightarrow N_2O$

→ N_2) (Knowles, 1982). This chain of reactions can be interrupted at each step depending on biological and kinetic factors (Carrey et al., 2013).

Both processes, the biotic Cr(VI) reduction and the denitrification can be heterotrophic or autotrophic depending on the use of an organic C or inorganic compound (e.g., sulphide or Fe(II)), respectively as electron donors. Therefore, since both reactions compete for the supply of the electron donors, the presence of NO_3^- can decrease the effectiveness of microbial Cr(VI) reduction (Middleton et al., 2003).

Isotope studies have been applied to discriminate between processes that imply an attenuation of Cr(VI) and NO_3^- concentrations by reduction processes and transport processes in the porous medium (dilution/dispersion) (Blowes, 2002; Berna et al., 2010; Wanner et al., 2012a, Margalef-Marti et al., 2019a). During the biotic or abiotic reduction of Cr(VI) to Cr(III), a kinetic isotope effect occurs since the lighter isotope, ^{52}Cr, reacts preferentially and therefore, the remaining dissolved Cr(VI) becomes enriched in the heavier isotope, ^{53}Cr (Ellis et al., 2002; Sikora et al., 2008; Kitchen et al., 2012; Basu et al., 2014).). Additionally, the Cr(III) species do not undergo rapid isotopic exchange with Cr(VI) species (Zink et al., 2010). Therefore, the calculation of this change in the isotope ratios, or isotope fractionation (ε), can be used to assess the natural or induced attenuation of Cr(VI) in contaminated groundwater (Izbicki et al., 2008; Berna et al., 2010; Raddatz et al., 2011; Wanner et al., 2012a; Heikoop et al., 2014). Likewise, during denitrification, as NO_3^- concentration decreases, the residual NO_3^- becomes enriched in the heavy isotopes (^{15}N and ^{18}O) (Aravena and Robertson, 1998; Fukada et al., 2003; Kendall et al., 2007; Mariotti et al., 1988). Experimental studies show that NO_3^- reduction occurring simultaneously with

100 Cr(VI) reduction can have a significant influence on the Cr(VI) isotope
101 fractionation (Ishibashi et al., 1990; Dichristina 1992; Garbisu et al., 1998;
102 Viamajala et al., 2002; Vatsouria et al. 2005; Han et al. 2010, 2012). Moreover,
103 isotope tracers have proven to be a powerful tool in identifying NO_3^- and Cr(VI)
104 sources in groundwater (Ellis et al., 2002; Otero et al., 2009).
105 At present, no case studies evaluate, through laboratory and field scale studies,
106 the coupled natural attenuation of hexavalent chromium and nitrates in
107 groundwater. The Matanza-Riachuelo River Basin (MRB) is the most populated
108 (>4 million people), industrialised and contaminated basin in Argentina (Zabala
109 et al., 2016). In several areas of the basin, the main source of water for human
110 and industrial supply is groundwater. Ceballos et al. (2018) detected that
111 groundwater, in some areas within MRB, is affected by both Cr(VI) (up to 5
112 mg/L) and NO_3^- (>100 mg/L) contamination. The main source of Cr(VI)
113 contamination is related to a chemical industry plant that operated from 1968 to
114 1990, producing bichromates, chromic acid, sulfuric acid and tannery products
115 (Salvador, 2013). During the operation period, the processing residues
116 containing Cr(VI) salts were disposed untreated into nearby unlined piles where
117 the dissolution of these waste salts promoted the migration of Cr(VI) through the
118 vadose zone into groundwater. The aim of the present study is to combine Cr
119 isotopes and N and O isotopes of dissolved nitrate for the purpose of identifying
120 natural attenuation processes of Cr(VI) and NO_3^- in groundwater. An implicit
121 primary goal is to determine, in laboratory experiments, using groundwater and
122 sediment from the studied area, the degree of isotope fractionation of Cr ($\varepsilon^{53}Cr$)
123 and of N ($\varepsilon^{15}N_{NO3}$) and O ($\varepsilon^{18}O_{NO3}$) during the simultaneous Cr(VI) and NO_3^-
124 reduction. The final goal is to assess the usefulness of the isotope approach to

study natural attenuation at field scale. The use of isotope tools to determine the extent of natural attenuation of Cr(VI) and NO_3^- in groundwater, serve as the basis for designing effective remediation strategies in the most exploited and contaminated aquifers in Argentina.

2. STUDY AREA

The MRB is located to the NE of the Buenos Aires province, Argentina (Figure 1A). The MRB is a hydrographic basin that covers an area of approximately 2,065 km^2 with very low slopes, forming a typical plain landscape. It consists of preferably continental sedimentary deposits. The main course is the Matanza River, which flows to the NE for 70 km before to be renamed Riachuelo about 15 km before discharging into the Río de la Plata. The area has a temperate climate with warm summers and cool winters. Average rainfall for the period 1906–2014 was 1100 mm/year (Scioli and Burgos 2015).

The MRB has its main source of water supply and industrial in two aquifer systems, the Upper aquifer of medium to low productivity with a variable water quality, and the Puelche Aquifer, of medium to high productivity and good water quality (Zabala et al., 2016). The Upper Aquifer holds the water table and receives natural recharge by infiltration of rainfall. Its thickness is around 40 m (Mancino et al., 2013) and consists of sandy-clayey-silts loess (Holocene), of homogeneous fine-grained loess and sandy loess (Pleistocene), and of interbedded carbonate (tosca). The Puelche Aquifer has a maximum thickness of 60 m consisting of quartz sands in the lower sandy section and silts and clays that are interbedded towards the top (Upper Pliocene to Pleistocene). These silty clay sediments behave as an aquitard of heterogeneous thickness but in

some sectors of the lower basin this aquitard does not exist because the sediments of the Upper Aquifer are in direct contact with the sands of the Puelche Aquifer. Due to the Puelche Aquifer not outcropping in the MRB, its recharge occurs directly from the Upper Aquifer by vertical filtration (Vives et al., 2013). The average annual recharge to the Upper Aquifer for the period 1906-2014 was 133 mm/year (Scioli and Burgos 2015). The groundwater discharges to surface water (streams, rivers) including to Río de la Plata. The two aquifers show similar piezometric patterns, in both of them regional groundwater flow is SW to NE (Vives et al., 2013). In the upper and middle parts of the basin, the water table surface reflects a strong relationship with the streams. The piezometric levels of the Upper and Puelche Aquifer respond simultaneously to seasonal recharge elevations and dry-season drawdowns, showing a strong connection of both aquifers (Zabala et., al 2016). Groundwater of the Upper Aquifer and the Puelche Aquifer has a similar chemical composition, generally of a Na-HCO_3 type in the area of study (Ceballos et al., 2018). The study area is located in San Ignacio neighbourhood, Jagüel town, at the lowest stretch of the Ortega Stream sub basin, in a tributary of the Matanza-Riachuelo River (Figure 1B). In this sector, the local flow direction of the Upper Aquifer would be conditioned by the Ortega stream, with a flow direction mainly of S-N / NW (Melián, 2014). A downward vertical hydraulic gradient from the Upper to the Puelche Aquifer has also been observed in the site of study (Ceballos et al., 2018). In the San Ignacio neighbourhood, the population does not have access to water supply and sanitation services. The residents have their own on-site solutions through septic tanks or pits. The drinking water supply is obtained from the municipal water trailer or purchased individually.

175

176 ## 3. METHODOLOGY

177 ### 3.1. Sampling of groundwater and soil

178 Groundwater samples were collected (September 2017) from three monitoring
179 wells belonging to the basin authority ACUMAR (samples P13, P28 and P29)
180 and nine private supply wells (samples P15, P21, P22, P26, P27, P31, P33 and
181 P34) (Figure 1B). Sample P28 was obtained from the Puelche Aquifer (well
182 depth of 40 m) while the rest of the samples were obtained from the Upper
183 aquifer (well depths from 15 to 20 m). The wells were purged three times the
184 volume of water in the column. Parameters such as electrical conductivity (EC),
185 temperature, pH and dissolved O_2 were measured in situ with a Multiparameter
186 PCS Testr 35 Series tester, using a flow cell to avoid contact with the
187 atmosphere. The samples were collected in polyethylene bottles after the wells
188 had been continuously pumped until the EC values became stabilised. A
189 volume of 30 mL was collected for non-purgeable dissolved organic carbon
190 (NPDOC) analysis in glass bottles previously combusted. These samples were
191 passed through a 0.45 µm nylon filter and acidified with 1 mL of HCl (2 N); the
192 bottles were sealed with Parafilm® to minimise any contact with air. A volume of
193 200 mL was collected for Cr(VI) analysis in polyethylene bottles. These samples
194 were filtered with a 0.45 µm membrane filter, then the pH was adjusted to 9 with
195 NaOH (1 N) and stored at +4ºC. Samples for the Cr isotope analyses were
196 collected in polyethylene bottles and stored at +4ºC until analysis. Samples for
197 the NO_3^- isotope analyses were filtered with a 0.22 µm filter (PTFE Teflon filter),
198 transferred into in 10 mL plastic vials and stored at -20 °C.
199 Soil samples were collected from a drilling downstream of the chemical industry

200 site near the ACUMAR P28 monitoring well (see Figure 1B). The drilling
201 reached 4 m whereas the water table was detected at 3 m depth. The sediment
202 was sampled between depths of 3 m and 4 m below the ground surface. These
203 soil samples were isolated from the atmosphere with polypropylene and stored
204 in the refrigerator at +4 ºC, until used in the batch experiments.
205
206 **3.2. Batch experiments**
207 The batch experiments aimed to determine the isotope fractionation of Cr(VI),
208 N-NO_3^- and O-NO_3^- during their reduction by organic carbon under different
209 scenarios. Three types of biostimulated microcosms were set up in 125 mL
210 crystal bottles sealed with butyl rubber septa and aluminium crimp under an
211 argon (Ar) headspace. The experiments were set up inside a glove box to avoid
212 any trace of dissolved O_2 and N_2. Each bottle contained sediment and
213 groundwater from the Upper aquifer. We used 75 mL of groundwater collected
214 from the P13 monitoring well, 15 g of sediment collected near the P28
215 monitoring well and added ethanol as external carbon source. Organic carbon
216 was selected to enhance Cr(VI) and NO_3^- reduction due to it is the main source
217 of electrons at field. Three series of parallel experiments were performed
218 according to Cr(VI) content (additional $K_2Cr_2O_7$ salt was added) and NO_3^-
219 concentration (groundwater NO_3^- concentration was 4.2 mM, no additional NO_3^-
220 was added). The experiment "BioCr" only contained Cr(VI) (0.2 mM), the
221 experiment "BioN" only contained NO_3^- (4.2 mM) and the experiment "BioCrN"
222 contained both species. For the "BioCr" experiment, the NO_3^- from groundwater
223 was previously removed by inducing denitrification through the addition of
224 ethanol as electron donor. All series included at least 10 replicates of

biostimulated microcosms. Control microcosms without ethanol "CtrlCrN" were carried out for the BioCrN experiments to check the contribution of the sediment on the Cr(VI) and NO_3^- reduction. Moreover, a set of blank microcosms containing only sediment and deionized water (DIW) was also performed to evaluate sediment leaching. The detailed content of each microcosm is shown in Table 1. For incubation, the bottles were wrapped with aluminium foil to avoid photodegradation processes and were maintained at room temperature (~ +24 ºC) with continuous orbital agitation. The biostimulated microcosms were sacrificed after fixed time spans according to previous laboratory tests (data not shown). The control microcosms were sacrificed at the end of the biostimulated experiment. The samples were immediately filtered with 0.22 µm nylon filters and stored at +4 ºC for further analysis. An aliquot for the NO_3^- isotopic analysis was stored at -20 ºC.

3.3. Analytical techniques

The Cr(VI), NO_3^-, nitrite (NO_2^-), ammonium (NH_4^+) and non-purgeable dissolved organic carbon (NPDOC) concentration was determined in all samples. The $\delta^{53}Cr$, the $\delta^{15}N_{NO3}$ and $\delta^{18}O_{NO3}$ were determined in all samples collected in the field and in a subset of samples of the laboratory experiments considered representative based on the Cr(VI) and NO_3^- concentrations.

Main anions (NO_3^-, SO_4^{2-}, Cl^- and NO_2^-) were analysed by high-performance liquid chromatography (HPLC) using a WATERS 515 HPLC pump with IC-PAC Anion columns and WESCAN and UV/VIS KONTRON detectors. The NH_4^+ was determined by colorimetry, Indophenol blue method (SP-830 plus Metertech). The NPDOC was measured by organic matter combustion (TOC 500

250 SHIMADZU). The dissolved Cr(VI) was determined within 24 h of sample
251 collection by using the diphenylcarbazide, SM 3500-Cr B method and a UV-Vis
252 spectrophotometer (SP-830 plus Metertech). Total dissolved Cr and trace
253 elements were determined by inductively coupled plasma mass spectrometry
254 analyses (ICP-MS, Perkin-Elmer Elan 6000) and inductively coupled plasma
255 optical emission spectrometry (ICP–OES, Perkin-Elmer Optima 3200 RL),
256 respectively, after acidifying the filtered samples (1% HNO_3).
257 The $\delta^{53}Cr$ analyses were performed following a slightly modified method from
258 Frei et al., (2009). An amount of water sample which would yield about 1 µg of
259 total Cr was pipetted into 23 mL Teflon beakers (Savillex ™) together with an
260 amount of a ^{50}Cr–^{54}Cr double spike so that a sample to spike ratio of ~3:1 (total
261 Cr concentrations) was achieved. The mixture was totally evaporated and 3 mL
262 of concentrated *aqua regia* was subsequently added. After 3 h with *aqua regia*
263 on a hot plate at 100 °C, the sample was again dried down. Then, the sample
264 was dissolved into 20 mL of ultrapure water (Milli Q®) and 0.5 mL of 1 N HCl, to
265 which 0.5 mL of a 0.5 M ammonium peroxydisulfate solution (puratronic®
266 quality) was added. The samples were then boiled for 1 hour with beaker lids
267 closed on a hot plate at 130 °C. This enabled the total oxidation of Cr to Cr(VI).
268 The solution was then passed over 2 ml pre-cleaned anion exchange resin
269 (DOWEX AG1X8; BioRad™). After rinsing with 5 mL of 0.1 N HCl, Cr(VI) was
270 reduced during 30 min on the columns, with 1 mL of 2 N HNO_3 to which three
271 drops of hydrogen peroxide were added. Cr(III) was then extracted with another
272 5 mL of the same 2 N HNO_3 hydrogen peroxide mixture into the 23 mL
273 Savillex™ beaker and subsequently dried down. The produced chromium
274 fraction was then purified, by passing the sample in 0.5 N HCl over a

275 miniaturized disposable pipette-tip extraction column, fitted with a bottom and a
276 top disposable PVC frit, which was charged with 300 µL of 200–400 mesh
277 cation resin (AGW-X12, BioRad™), thus employing the slightly modified
278 extraction procedure, published by Trinquier et al. (2009) and Bonnand et al.
279 (2011). The yield of this mini-column extraction and purification step is usually
280 ~70%. Samples were loaded onto Re filaments with a mixture of 3 µL silica gel,
281 0.5 µL 0.5 mol/L of H_3BO_3 and 0.5 µL 0.5 mol/L of H_3PO_4. The samples were
282 statically measured on an IsotopX "Phoenix" multicollector thermal ionization
283 mass spectrometer (TIMS) at the Department of Geoscience and Natural
284 Resource Management, University of Copenhagen, at temperatures between
285 1050 and 1200 °C, aiming at beam intensity at atomic mass unit (AMU) 52.9407
286 of 30–60 mV. Each load was analysed 2–4 times. Titanium, vanadium and iron
287 interferences with Cr isotopes were corrected by comparing with $^{49}Ti/^{50}Ti$,
288 $^{50}V/^{51}V$ and $^{54}Fe/^{56}Fe$ ratios. The final isotope composition of each sample was
289 determined as the average value of repeated analyses and reported, relatively
290 to the certified SRM 979.
291 The $\delta^{15}N_{NO3}$ and $\delta^{18}O_{NO3}$ were determined following the cadmium reduction
292 method (McIlvin and Altabet, 2005; Ryabenko et al., 2009). Then, the N_2O was
293 analysed using a Pre-Con (Thermo Scientific) coupled to a Finnigan MAT 253
294 Isotope Ratio Mass Spectrometer (IRMS, Thermo Scientific). Isotopic analyses
295 of NO_3^- were prepared at the laboratory of the MAiMA-UB research group and
296 analysed at the Centres Científics i Tècnològics of the Universitat de Barcelona
297 (CCiT-UB).
298 The isotopic notation is expressed in terms of δ per mil relative to the
299 international standards (Equation 1):

$\delta = \frac{R_{sample}-R_{standard}}{R_{standard}}$ where R = $^{53}Cr/_{52}Cr$ and $^{15}N/_{14}N$, respectively

Equation 1

NIST SRM 979 for $\delta^{53}Cr$, Vienna Standard Mean Oceanic Water (V-SMOW) for $\delta^{18}O$ and Atmospheric N_2 (AIR) for $\delta^{15}N$. According to Coplen, (2011), several international and laboratory (CCiT) standards were interspersed among samples for the normalisation of the results (Table 2). The standard deviation reproducibility of the samples was ± 0.08 ‰ for $\delta^{53}Cr$, ±1.0 ‰ for $\delta^{15}N_{NO3}$, ±1.5 ‰ for $\delta^{18}O_{NO3}$.

3.4. Isotope data calculations

The isotope fractionation (ε), under closed system conditions, can be calculated using the Rayleigh distillation equation (Equation 2). Thus, ε can be obtained from the slope of the linear correlation between the natural logarithm of the substrate remaining fraction ($Ln(C_{residual}/C_{initial})$, where C refers to the analyte concentration) and the determined isotope ratios ($Ln(R_{residual}/R_{initial})$, where R = (δ+1).

$$Ln\left(\frac{R_{residual}}{R_{initial}}\right) = \varepsilon \times Ln\left(\frac{C_{residual}}{C_{initial}}\right) \qquad \text{Equation 2}$$

The percentages of the Cr(VI) reduction and denitrification at field scale can be determined by using the isotopic composition of the samples and the ε values obtained at laboratory scale using Equation 3 (Ellis et al., 2002; Berna et al., 2010; Raddatz et al., 2011; Torrentó et al., 2011; Carrey et al., 2013).

$$(\%) = \left[1 - e^{((\delta residual - \delta initial)/\varepsilon)}\right] \times 100 \qquad \text{Equation 3}$$

4. RESULTS AND DISCUSSION

The chemical and isotopic data of the samples obtained from the laboratory batch experiments and the samples collected at field are summarised in Tables 3 and 4, respectively.

4.1. Batch experiments: Cr(VI) and NO_3^- reduction by organic matter.

In the blank experiments uniquely containing sediment and DIW, 0.01 mM NO_3^- was detected, NO_2^- was below 0.006 mM, NH_4^+ below 0.03 mM and NPDOC reached up to 0.87 mM. These results suggest a possible lixiviation of N compounds and organic C from the sediment. However, since the NO_3^- concentration in groundwater was much higher (4.2 mM), the amount of lixiviated N was considered negligible. Control experiments without ethanol (CtrlCrN) showed no significant variation in the Cr(VI) and NO_3^- concentrations when incubated (38 to 263 hours) with groundwater and sediment collected at the study site (Table 3). The NO_2^- and NH_4^+ concentration in these microcosms were below 0.005 mM, while NPDOC reached up to 0.33 mM. Therefore, despite NPDOC lixiviated from the sediment, it was not able to trigger neither NO_3^- nor Cr(VI) attenuation.

In the BioCr experiment, the initial Cr(VI) content of 0.19 mM started to decrease after approximately 50 h from the beginning of the experiment and was completely reduced during approximately 130 hours (Figure 2A). The $\delta^{53}Cr$ increased from +0.05 ‰ to +3.4 ‰. This increase coincides with the decrease in Cr(VI) concentration, which would indicate that Cr reduction was occurring (Table 3). In the BioN experiment, NO_3^- started to decrease after approximately

18 h from the beginning of the experiment and was completely eliminated within 31 h (Figure 2B). After the onset of NO_3^- attenuation, NO_2^- started to accumulate reaching 1.7 mM at 28 h and then decreased until being completely reduced in approximately 40 h. Transient NO_2^- accumulation is commonly observed in denitrification experiments and is usually influenced by the initial growth of denitrifying bacteria and the induction of the nitrite reductase (Betlach and Tiedje, 1981; Carrey et al., 2013; Margalef-Marti et al., 2019b). The measured NH_4^+ concentration was below 0.02 mM. The amount of NH_4^+ detected could be derived from the sediment leaching and allowed to discard other reactions such as the dissimilatory NO_3^- reduction to NH_4^+ (DNRA) as responsible for NO_3^- reduction. The $\delta^{15}N_{NO3}$ increased from +11.2 ‰ to +56.5 ‰ and $\delta^{18}O_{NO3}$ from +7.1 ‰ to + 65.7 ‰ as NO_3^- concentration decreased (Table 3). The enrichment in the heavy isotopes in the remaining substrate, both in the case of Cr(VI) and NO_3^- attenuation mediated by the ethanol addition, is consistent with bacterial heterotrophic activity.

In the BioCrN experiment, the initial content of Cr(VI) (0.2 mM) started to decrease after approximately 48 h from the beginning of the experiment and was completely reduced in approximately 130 h (Figure 2A). In combination with the Cr(VI) reduction, the $\delta^{53}Cr$ of the remaining substrate increased from +0.05 ‰ to +3.3 ‰ (Table 3). Simultaneously, the initial NO_3^- content started to decrease after approximately 48 h from the beginning of the experiment and was completely eliminated in less than 100 h (Figure 2B). After the onset of NO_3^- attenuation, NO_2^- started to accumulate reaching 2.0 mM at about 70 h and then decreased until being completely reduced in approximately 120 h. The measured NH_4^+ concentration was below 0.01 mM. As in the case of the BioN

373 experiment, NH_4^+ observed could be derived from the sediment leaching and
374 allowed to discard other NO_3^- reducing reactions such as DNRA. Under these
375 conditions, the $\delta^{15}N_{NO3}$ increased from +11.2 ‰ to +64.8 ‰ and $\delta^{18}O_{NO3}$ from
376 +7.1 ‰ to + 72.2 ‰ (Table 3). The enrichment in the heavy isotopes of the
377 remaining Cr(VI) and NO_3^- during its concomitant reduction by ethanol is again
378 consistent with the bacterial heterotrophic activity.
379 The comparison of the BioCr and BioN experiments with the BioCrN
380 experiments shows that while Cr(VI) reduction rate was not affected by
381 denitrification, NO_3^- attenuation was slower in the presence of Cr(VI). Compared
382 to the BioN experiments, in the BioCrN experiments the NO_3^- concentration
383 decrease started 30 hours later (48 hours instead of 18) and the reduction of
384 both NO_3^- and NO_2^- was completed 80 hours later (120 hours instead of 40).
385 Therefore, the presence of Cr(VI) slowed down denitrification, but did not
386 completely inhibit it. The most likely explanation is that the presence of Cr(VI)
387 promotes a certain toxicity to the denitrifying bacterial species stimulated from
388 the groundwater and sediment collected at the study site, while NO_3^- seems to
389 have no effect on the stimulated Cr(VI) reducing species. The inhibition of NO_3^-
390 reduction by Cr(VI) was previously observed by Kourtev et al., (2009). These
391 authors found a decrease in NO_3^- reduction coupled with an increase of Cr(VI)
392 content when using lactate as organic C source. The authors also observed a
393 decreased bacterial growth yield when increasing the Cr(VI) concentration.
394 These results suggest that Cr(VI) toxicity to NO_3^- reducing microorganisms
395 might be dependent on its concentration, the specific species involved, and the
396 electron donors employed.
397

4.2. Batch experiments: Isotopic fractionation.

Batch experiments were performed to determine the $\varepsilon^{53}Cr$, $\varepsilon^{15}N_{NO3}$ and $\varepsilon^{18}O_{NO3}$ under the three different conditions tested (BioCr, BioN and BioCrN). The calculations are shown in Figure 3 and a summary of the obtained values including the $\varepsilon^{15}N/\varepsilon^{18}O$ calculation is presented in Table 5.

In both the BioCr and BioCrN experiments (Figure 3A and 3B, respectively), two different slopes were observed, and consequently two $\varepsilon^{53}Cr$ values were calculated. During the Cr(VI) reduction in the absence of NO_3^- (BioCr), the first stage is defined by the samples with a higher Cr(VI) content (0.21 to 0.07 mM) and shows a $\varepsilon^{53}Cr$ of -1.4 ‰ (r^2 = 0.90), while the second stage applies to samples with lower Cr(VI) concentrations (0.05 to 0.002 mM) and reveals a $\varepsilon^{53}Cr$ of -0.2 ‰ (r^2 = 0.45). During the Cr(VI) reduction in the presence of denitrification (BioCrN), a similar pattern is observed. The first stage is defined by the samples with a higher Cr(VI) content (0.21 to 0.06 mM) and implies a $\varepsilon^{53}Cr$ of -1.8 ‰ (r^2 = 0.99), while the second stage applies to samples with lower Cr(VI) concentrations (0.05 to 0.03 mM) and reveals a $\varepsilon^{53}Cr$ of -0.9 ‰ (r^2 = 0.44). Likewise, Chen et al. (2019) assessed the $\varepsilon^{53}Cr$ during the Cr(VI) reduction under various conditions (temperatures from 18 to 34 ºC and pH from 6.0 to 7.2, presence and absence of nitrate) and also found two-stage trends. These authors, upon the tested conditions, obtained a $\varepsilon^{53}Cr$ during the first stage ranging from -2.6 ‰ to -2.8 ‰, while in the second stage the values were between -1.0 ‰ and -1.1 ‰. Hence, a lower isotope fractionation (in absolute ε values) was found for the second stage, when Cr(VI) concentrations were lower, and yielded values similar to the isotope fractionation obtained in the present BioCr and BioCrN experiments. Furthermore, these authors, suggested

423 that the decreased Cr(VI) bioavailability when the reduction progresses could
424 mask the isotopic fractionation. However, in other biotic Cr(VI) reduction
425 experiments, such two-stage trends were not observed (Basu et al., 2014;
426 Sikora et al., 2008). If indeed, the Cr(VI) isotope fractionation occurs in two
427 stages, the use of a ε^{53}Cr for a single stage to estimate the Cr(VI) reduction at
428 field-scale, could underestimate or overestimate the extent of the reaction.
429 Therefore, two-stage pattern could have implications when using ε^{53}Cr values
430 calculated from laboratory experiments to quantify the natural or induced Cr(VI)
431 reduction, since different ε^{53}Cr values should be used depending on Cr(VI)
432 concentration.
433 In the present study, when Cr(VI) was concomitantly reduced with NO_3^-
434 (BioCrN), a slightly higher ε^{53}Cr (absolute value) was obtained compared to the
435 BioCr batch (Cr(VI) reduced in the absence of NO_3^-), although the reduction
436 rate was similar. However, these results differ from those reported by Han et al.
437 (2012). These authors found a lower ε^{53}Cr value (–0.4 ‰) under denitrifying
438 conditions compared to the value obtained in the absence of NO_3^- (-2 ‰). On
439 the other hand, Chen et al. (2019) obtained similar ε^{53}Cr values with presence (-
440 2.4 ‰ and -0.9 ‰) and absence (-2.7 ‰ and -1.1 ‰) of NO_3^-. Therefore, it is
441 clear that the presence of NO_3^- has an influence on the Cr(VI) isotope
442 fractionation, and when calculating Cr(VI) reduction rates from field-based data,
443 the ε^{53}Cr values employed should take into account the presence or absence of
444 NO_3^-.
445 As to the biotic Cr(VI) reduction in absence of NO_3^-, Basu et al. (2014) reported
446 ε^{53}Cr in a range of -2.2 ‰ a -3.1 ‰ for pure culture experiments using different
447 bacterial species and Sikora et al. (2008) found a ε^{53}Cr of -1.8 ‰ when testing

448 10 mM lactate and between -4.1 and -4.5 ‰ when testing lactate below 100 µM
449 for the reduction. These results suggest that the microbial species and electron
450 donor concentration involved in the Cr(VI) reduction could have an influence on
451 the resulting isotope fractionation. For the abiotic Cr(VI) reduction, Ellis et al.
452 (2002) found a $\varepsilon^{53}Cr$ = -3.5 ‰ when using magnetite as the electron donor and
453 Kitchen et al. (2014) and Døssing et al. (2011) found $\varepsilon^{53}Cr$ in a range of -2.9 ‰
454 and -4.9 ‰ when using Fe(II) or organic acids at different pH. These results
455 suggest that no significant isotopic fractionation differences are found between
456 biotic and abiotic Cr(VI) reactions.
457 The $\varepsilon^{15}N_{NO3}$ and $\varepsilon^{18}O_{NO3}$ values for the BioN and BioCrN experiments were
458 calculated together. Despite the BioN experiment showing a higher NO_3^-
459 reduction rate, a similar slope with a good correlation is obtained for both
460 experiments (Figure 3C). The $\varepsilon^{15}N_{NO3}$ and $\varepsilon^{18}O_{NO3}$ values are -23.9 ‰ and -25.7
461 ‰, respectively (Figure 3C). These values and the resulting $\varepsilon^{15}N/\varepsilon^{18}O$ (0.9) are
462 within the data range reported in the literature for denitrifying processes
463 (Granger et al., 2008; Knöller et al., 2011; Grau-Martínez et al., 2017 and
464 references therein). The obtained $\varepsilon^{15}N_{NO3}$ and $\varepsilon^{18}O_{NO3}$ values in the present
465 experiments can be employed to quantify the natural attenuation of NO_3^- at the
466 study site.
467

468 **4.3. Natural attenuation of Cr(VI) and NO_3^- in the study area.**

469 Hydrochemical data for the 11 groundwater samples collected in the San
470 Ignacio neighbourhood show pH values between 7.1 and 8.1, and electric
471 conductivity (EC) varied from 992 µS/cm to 2060 µS/cm (Table 4). The Cr(VI)
472 concentrations range from below detection limit to 0.041 mM, next and

473 downstream of the chemical industry plant. The NO_3^- was detected in all
474 samples from the studied area and concentrations vary between 0.5 mM and
475 3.9 mM, with an average of 1.4 mM. Likewise, the NPDOC varies between 0.08
476 mM and 0.2 mM. The presence of both contaminants in the deeper aquifer is
477 linked to the hydraulic conductivity of the aquitard, because it controls the
478 hydraulic connectivity between the Upper and the Puelche Aquifer.
479 The $\delta^{53}Cr$ in groundwater varies between +1.2 ‰ and +3.4 ‰, with an average
480 value of +2.8 ‰. The spatial distribution of the $\delta^{53}Cr$ values indicates a
481 downstream increase along the axis of the plume, following the groundwater
482 flow line (Figure 4). Near the source of Cr(VI), the $\delta^{53}Cr$ value is +1.2 ‰ and
483 values increase to +3.4 ‰ 200 m downstream. The observed increase in $\delta^{53}Cr$
484 values downstream from the Cr(VI) source suggests that Cr(VI) attenuation is
485 occurring due to biotic reduction.
486 The isotope values of dissolved nitrate indicate the occurrence of NO_3^-
487 reduction, evidenced by an enrichment in the heavy isotopes that ranged from
488 +10.6‰ to +22.8‰ for the $\delta^{15}N$ and from +6.1‰ to +12.7‰ for the $\delta^{18}O$ (Table
489 4). A positive linear correlation between $\delta^{15}N_{NO3}$ and $\delta^{18}O_{NO3}$ with a slope of
490 0.51 (r^2 = 0.79) is exhibited by the analysed samples (Figure 6). These results
491 are in the range of values reported in the literature for denitrification processes
492 in groundwater (Aravena and Robertson, 1998; Kendall et al., 2007). In the
493 samples obtained from the monitoring wells, dissolved O_2 concentrations vary
494 between 0.02 and 0.2 mM, which would indicate inadequate conditions for
495 denitrification according to the required O_2 concentration below 0.1 mM
496 reported by Cey et al., (1999). However, denitrification has also been found at
497 higher dissolved O_2 concentrations (Otero et al., 2009). On the other hand, the

498 samples collected at the study site with higher $\delta^{53}Cr$ also are characterized by
499 higher values of $\delta^{15}N_{NO3}$ and $\delta^{18}O_{NO3}$. For example, sample P29 yielded a $\delta^{53}Cr$
500 of +3.4‰, $\delta^{15}N_{NO3}$ of +22.8‰ and $\delta^{18}O_{NO3}$ of +12.7‰, which are the highest
501 measured isotope values for these compounds (see also samples P31, P21 and
502 P22 in Table 4). Therefore, we confirmed that Cr(VI) reduction can occur
503 simultaneously with denitrifying processes. Furthermore, since the NO_3^- isotope
504 composition of the samples collected in the field are within the defined range for
505 wastewater NO_3^- (Figure 6), we also identify that the source of NO_3^- is
506 potentially related with septic systems leakage. On the other hand, septic
507 systems leakage could be a source of NPDOC in groundwater and therefore,
508 denitrification and Cr(VI) reduction could be related to the oxidation of organic
509 matter.
510
511 **4.4. Estimation of Cr(VI) and NO_3^- reduction percentage in**
512 **contaminated groundwater**
513 In the calculation of the percentage of Cr(VI) attenuation, we used the sample
514 P34 as representative for the initial value of Cr(VI) concentration and isotope
515 composition (Table 4), because it is the sample with the highest Cr(VI) content
516 and because the well is located very close to the source of contamination. The
517 $\varepsilon^{53}Cr$ values we used are those calculated in the BioCrN experiments (stage I =
518 -1.8 ‰ and stage II = -0.98 ‰), since we observed the simultaneous Cr(VI) and
519 NO_3^- reduction at field. Calculated Cr(VI) attenuation percentages in
520 groundwater samples by using the $\varepsilon^{53}Cr$ from stage I vary between 60 % and 70
521 %, but when using the $\varepsilon^{53}Cr$ value from stage II, the attenuation of Cr(VI) is
522 calculated at much higher percentages (80% and 90%). Using the $\varepsilon^{53}Cr$ values

523 from stage I, in sample P33, extracted from the well located closest to the
524 source (see Figure 1), we calculate that ~60 % of the original Cr(VI) was
525 eliminated by reduction. In samples P21 and P22, located in the central part of
526 the plume axis, these values are 63 % and 62 %, respectively. For samples
527 P28, P29 and P31, located in the distal part of the plume, the reduction
528 percentage is 64 %, 69 % and 66 %, respectively. On the other hand, applying
529 the ε^{53}Cr value from stage II, for sample P33, the Cr(VI) attenuation is 84 %. For
530 samples P21 and P22 the attenuation is 86 % and 85 %, respectively, and
531 values for samples P28, P29 and P31 imply an attenuation percentage of 87 %,
532 91 % and 89 %, respectively. Figure 5 shows the δ^{53}Cr *vs* the Ln(Cr(VI)) of the
533 studied samples together with two Cr reduction models calculated applying the
534 Rayleigh equation. Sample P28, located downstream of the source, and with
535 high Cr (V) concentration is located in the theoretical denitrification line obtained
536 from applying stage I. However, sample P31 with a lower Cr (VI) concentration
537 is located in the theoretical line obtained by applying the slope II model,
538 showing a higher percentage of degradation. On the other hand, samples P33,
539 P21, P22 and P29 have much lower Cr (VI) concentrations but similar isotopic
540 composition. These samples are located in the theoretical line of dilution,
541 starting from a sample with δ^{53}Cr and Cr (VI) concentration similar to P28 or
542 P31, suggesting that the attenuation of Cr (VI) in these samples would be
543 partially linked to a process of mixing with uncontaminated groundwater and not
544 only to reduction of Cr(VI) to Cr(III).
545 With regards to NO_3^- attenuation, the sample with the highest NO_3^- content is
546 assumed as initial value (P13) and ε values calculated from the BioN and
547 BioCrN experiments (-24.1‰ for ε^{15}N and -24.3‰ for ε^{18}O) were selected. The

548 lower slope between $\delta^{18}O\text{-}NO_3^-$ and $\delta^{15}N\text{-}NO_3^-$ obtained for the field samples
549 (0.5 (r^2 = 0.82)) with respect to the batch experiments (1.0 (r^2 = 0.95)) (Figure 6)
550 agrees with reported slopes of nearly 0.5 for field scale studies and nearly 1.0
551 for laboratory studies (Carrey et al., 2013; Critchley et al., 2014; Otero et al.,
552 2009; Wunderlich et al., 2012). The main reason that could cause this flatter
553 slope in field-based data sets, is the oxidation of the intermediates NO_2^- and/or
554 NH_4^+ to NO_3^- (Granger and Wankel, 2016; Wunderlich et al., 2013; Margalef-
555 Marti et al., 2019a). According to the denitrification percentage line drawn from
556 the laboratory results, most of the samples collected in the field imply an
557 approximate NO_3^- attenuation of 20 %, while three samples (P21, P34 and P29)
558 yield a higher attenuation (approximately 30 %) (Figure 6). Overall,
559 denitrification is taking place in the basin, but it cannot remove NO_3^- completely
560 from groundwater. It should be noted that, according to the ε values calculated
561 in laboratory experiments, for the studied groundwater samples, the natural
562 attenuation of Cr(VI) is considerably larger than the natural attenuation of NO_3^-.
563 These high percentages of attenuation could explain the low concentrations of
564 NPDOC detected in the groundwater samples at the study site.
565 The results obtained in the present study can be useful for future studies aiming
566 to evaluate the Cr(VI) and NO_3^- degradation by using isotope tools in
567 contaminated groundwater with these two compounds. Previous studies applied
568 isotopes to evaluate the natural or induced attenuation of Cr(VI) (Novak et al.,
569 2017; Economou-Eliopoulos et al., 2014; Heikoop et al., 20104; Berna et al.,
570 2010) and NO_3^- (Critchley et al., 2014; Margalef-Marti et al., 2019a; Otero et al.,
571 2009; Vidal-Gavilan et al., 2013) at field. However, to the best of our knowledge
572 no studies have reported an estimation of the percentage of degradation Cr(VI)

573 and NO_3^- when found simultaneously in contaminated aquifers and none of the
574 aforementioned studies considered the two-stage isotopic fractionation of
575 Cr(VI). To avoid over or underestimation of the percentage of degradation of the
576 two contaminants at field, this two stages Cr(VI) isotopic fractionation and the
577 NO_3^- reduction rate decreases in the presence of Cr(VI) must be considered
578 when designing laboratory experiments to calculate ε values. Furthermore,
579 hydrogeological and biochemical effects such as mixing of water from different
580 sources or NO_2^- reoxidation to NO_3^-, among many others, have to be taken into
581 account to interpret field-scale results. Due to these effects, the percentages
582 obtained from isotope data must be considered estimation, not a precise
583 calculation (Margalef-Marti et al., 2019a).
584

585 **5. CONCLUSIONS**

586 The isotope analyses of Cr(VI) and NO_3^- allowed to evaluate the contribution of
587 the natural attenuation processes in the evolution of these pollutants'
588 concentrations in the groundwater at the studied site of the MRB. The results of
589 our laboratory experiments evidence a concomitant Cr(VI) reduction with
590 denitrification. The Cr(VI) reduction rate is not affected by the presence of NO_3^-,
591 but NO_3^- attenuation is slower in the presence of Cr(VI). The $\varepsilon^{53}Cr$ produced by
592 the reduction of Cr(VI) to Cr(III) follows a two stage trend. A higher isotope
593 fractionation (-1.4 ‰ and -1.8 ‰ in absence/presence of NO_3^- respectively) was
594 found for the first stage compared to the second stage (-0.2 ‰ and -0.9 ‰ in
595 absence/presence of NO_3^- respectively). The presence of NO_3^- did not affect
596 notably the $\varepsilon^{53}Cr$, although the reduction rate was different. On the other hand,
597 we obtained equal $\varepsilon^{15}N_{NO3}$ and $\varepsilon^{18}O_{NO3}$ values (-23.9 ‰ and -25.7 ‰,

598 respectively) for the experiments with or without Cr(VI).

599 In a site of MRB, the δ^{53}Cr values of the studied samples increase downstream
600 of the Cr(VI) source following a flow line, suggesting that isotope fractionation
601 occurs along the plume. Using the ε^{53}Cr obtained at the laboratory, the
602 calculated Cr(VI) attenuation at the study site varies between 60-70%, or
603 between 85-90% when ε^{53}Cr from stage I or II are respectively applied. Besides,
604 the isotope results allowed identifying dilution in those samples with lower Cr
605 concentration. On the other hand, the percentage of NO_3^- attenuation in
606 groundwater samples varies between approximately 20% and 30%. Hence,
607 although Cr(VI) and NO_3^- are reduced concomitantly from the groundwater of
608 the San Ignacio neighbourhood, the natural attenuation of Cr(VI) is considerably
609 larger than that of NO_3^-.

610 The isotope methods used have made it possible to determine the degradation
611 of contaminants and confirmed that concentration changes of contaminants are
612 not exclusively due to dilution. Although with some uncertainty, we were able to
613 calculate attenuation percentages of these contaminants in the contaminated
614 basin studied which indicate a rather effective neutralization of otherwise toxic
615 Cr(VI) in the groundwaters. These results provided a basis for planning an
616 efficient management of the contaminated aquifer in the most populated and
617 industrialized basin of Argentina.

618

619 **ACKNOWLEDGEMENTS**

620 This research was supported by the Instituto de Hidrología de Llanura “Dr.
621 Eduardo J. Usunoff” (IHLLA) and by IDAEA-CSIC as part of the programme
622 EMHE “Enhancing Mobility between Latin-American and Caribbean countries

and Europe". We thank the IHLLA technic staff for their assistance in water sampling and Ms. M. F. Altolaguirre, B.S., and Ms. O. Floriani, B.S., for assisting in the logistics of manipulation and conservation of samples. This research is also supported by the project PACE-ISOTEC (CGL2017-87216-C4-1-R), financed by the Spanish Government and AEI/FEDER from the UE, and the project MAG (2017 SGR 1733) from the Catalan Government. We also thank the Centres Científics i Tecnològics of the Universitat de Barcelona for its analytical support.

REFERENCES

Amiri, H., Zare, M., and Widory, D., 2015. Assessing sources of nitrate contamination in the Shiraz urban aquifer (Iran) using the $\delta^{15}N$ and $\delta^{18}O$ dual-isotope approach. Isotopes in environmental and health studies, 51(3), 392-410.

Aravena, R., Robertson, W.D., 1998. Use of multiple isotope tracers to evaluate denitrification in ground water: study of nitrate from a large flux septic system plume. Ground Water 36, 975–982.

Aravena, R., Evans, M. L., & Cherry, J. A., 1993. Stable isotopes of oxygen and nitrogen in source identification of nitrate from septic systems. Groundwater, 31(2), 180-186.

Barford, C. C., Montoya, J. P., Altabet, M. A., and Mitchell, R. 1999. Steady-state nitrogen isotope effects of N2 and N2O production in Paracoccus denitrificans. Appl. Environ. Microbiol., 65(3), 989-994.

Basu, A., Johnson, T. M., and Sanford, R. A., 2014. Cr isotope fractionation

factors for Cr (VI) reduction by a metabolically diverse group of bacteria. Geochimica et Cosmochimica Acta, 142, 349-361.

Basu, A., and Johnson, T., 2012. Determination of hexavalent chromium reduction using Cr stable isotopes: Isotopic fractionation factors for permeable reactive barrier materials. Environmental Science & Technology, 46, 5353-5360.

Bellú, S., García, S., González, J., Atria, A., Sala, L., Signorella, S., 2008. Removal of Chromium (VI) and Chromium (III) from aqueous solution by grainless stalk of corn. Separation Science and Technology, 43, 3200-3220.

Berna, E. C., Johnson, T. M., Makdisi, R. S., and Basu, A., 2010. Cr stable isotopes as indicators of Cr (VI) reduction in groundwater: a detailed time-series study of a point-source plume. Environmental science & technology, 44(3), 1043-1048.

Betlach, M.R., Tiedje, J.M., 1981. Kinetic Explanation for Accumulation of Nitrite, Nitric Oxide, and Nitrous Oxide during Bacterial Denitrification. Appl. Environ. Microbiol. 42, 1074–1084. https://doi.org/Article

Blowes, D., 2002. Tracking hexavalent Cr in groundwater. Science, 295, 2024-2025.

Blowes, D. W., Ptacek, C. J., Benner, S. G., McRae, C. W., Bennett, T. A., Puls, R. W., 2000. Treatment of inorganic contaminants using permeable reactive barriers. Journal of Contaminant Hydrology, 45(1-2), 123-137.

Bonnand, P., Parkinson, I.J., James, R.H., Karjalainen, A.-M., Fehr, M.A., 2011.

671 Accurate and precise determination of stable Cr isotope compositions in
672 carbonates by double spike MC-ICP-MS. J. Anal. At. Spectrom. 26:528.
673 http://dx.doi.org/10.1039/c0ja00167h.

674 Böttcher, J., Strebel, O.L., Voerkelus, S., Schmidt, H.L., 1990. Using isotope
675 fractionation of nitrate-nitrogen and nitrate-oxygen for evaluation of
676 microbial denitrification in sandy aquifer. J. Hydrol. 144, 413–424.

677 Carrey, R., Rodríguez-Escales P., Soler, A., Otero, N., 2018. Tracing the role of
678 endogenous carbon in denitrification using wine industry by-product as
679 an external electron donor: Coupling isotopic tools with mathematical
680 modelling. Journal of Environmental Management 207, 105-115.

681 Carrey, R., Otero, N., Vidal-Gavilan, G., Ayora, C., Soler, A., Gomez-Alday, J.J.,
682 2014a. Induced nitrate attenuation by glucose in groundwater: flow-
683 through experiment. Chem. Geol. 370 (0), 19-28.

684 Carrey, R., Otero, N., Soler, A., Gómez-Alday, J.J., Ayora, C., 2013. The role of
685 lower Cretaceous sediments in groundwater nitrate attenuation in central
686 Spain: column experiments. Appl. Geochem. 32, 142–152.

687 Casciotti, K.L., Sigman, D.M., Hastings, M.G., Böhlke, J.K., Hilkert, A.,
688 2002.Measurement of the oxygen isotopic composition of nitrate in
689 seawater and freshwater using the denitrifier method. Anal. Chem. 74
690 (19), 4905–4912.

691 Ceballos, E., Bea, S. A., Sanci, R., 2018 Applying reactive transport modeling in
692 a chromium contaminated site in the Matanza-Riachuelo Basin, Buenos
693 Aires, Argentina. International Journal of Environment and Health. Vol. 9,

694 No. 1.

695 Cey, E. E., Rudolph, D. L., Aravena, R., Parkin, G. 1999. Role of the riparian
696 zone in controlling the distribution and fate of agricultural nitrogen near a
697 small stream in southern Ontario. Journal of Contaminant Hydrology,
698 37(1-2), 45-67.

699 Chen, G., Han, J., Mu, Y., Yu, H., and Qin, L. 2019. Two-stage chromium
700 isotope fractionation during microbial Cr (VI) reduction. Water research,
701 148, 10-18.

702 Chen, J.M., Hao, O.J., 1998. Microbial chromium (VI) reduction. Critical
703 Reviews in Environmental Science and Technology, 28: 219-251.

704 Cheng, Y., Yan, F., Huang, F., Chu, W., Pan, D., Chen, Z., Zheng, J., Yu, M., Lin,
705 Z., Wu, Z., 2010. Bioremediation of Cr (VI) and immobilization as Cr (III)
706 by Ochrobactrum anthropi. Environmental Science & Technology, 44:
707 6357-6363.

708 Cheung, K.H., Gu, J.D., 2007. Mechanism of hexavalent chromium
709 detoxification by microorganisms and bioremediation application
710 potential: A review. International Biodeterioration & Biodegradation, 59: 8-
711 15.

712 Coplen, T.B., 2011. Guidelines and recommended terms for expression of
713 stable-isotope-ratio and gas-ratio measurement results. Rapid Commun.
714 Mass Spectrom. 25, 2538–2560. https://doi.org/10.1002/rcm.5129

715 Critchley, K., Rudolph, D.L., Devlin, J.F., Schillig, P.C., 2014. Stimulating in situ
716 denitrification in an aerobic, highly permeable municipal drinking water

717 aquifer. J. Contam. Hydrol. 171, 66–80.

718 Dichristina, T. J. 1992. Effects of nitrate and nitrite on dissimilatory iron
719 reduction by Shewanella putrefaciens 200. Journal of bacteriology,
720 174(6), 1891-1896.

721 Davis, A., and Olsen, R. L. 1995. The geochemistry of chromium migration and
722 remediation in the subsurface. *Groundwater*, *33*(5), 759-768.

723 De Beer, D. I. R. K., Schramm, A., Santegoeds, C. M., & Kuhl, M., 1997. A nitrite
724 microsensor for profiling environmental biofilms. Applied and
725 Environmental Microbiology, 63(3), 973-977.

726 Døssing, L. N., Dideriksen, K., Stipp, S. L. S., Frei, R., 2011. Reduction of
727 hexavalent chromium by ferrous iron: a process of chromium isotope
728 fractionation and its relevance to natural environments. Chemical
729 Geology, 285(1-4), 157-166.

730 Economou-Eliopoulos, M., Frei, R., Atsarou, C., 2014. Application of chromium
731 stable isotopes to the evaluation of Cr(VI) contamination in groundwater
732 and rock leachates from central Euboea and the Assopos basin
733 (Greece). Catena, 122, 216-228.

734 Ellis, A., Johnson, T and Bullen, T.D., 2002. Chromium isotopes ratios and the
735 fate of Chromium in the environment. Science, 295, 2060-2062.

736 Farmer, J. G., Thomas, R. P., Graham, M. C., Geelhoed, J. S., Lumsdon, D. G.,
737 Paterson, E., 2002. Chromium speciation and fractionation in ground and
738 surface waters in the vicinity of chromite ore processing residue disposal
739 sites. Journal of Environmental Monitoring, 4(2), 235-243.

Fernández-Nava, Y., Marañón, E., Soons, J., Castrillón, L., 2010. Denitrification of high nitrate concentration wastewater using alternative carbon sources. J. Hazard. Mater. 173, 682–688.

Frei, R., Gaucher, C., Poulton, S.W., Canfield, D.E., 2009. Fluctuations in Precambrian atmospheric oxygenation recorded by chromium isotopes. Nature 461, 250–253

Fukada, T., Hiscock, K., Dennis, P.F., Grischek, T., 2003. A dual isotope approach to identify denitrification in groundwater at a river-bank infiltration site. Water Res. 37, 3070–3078.

Gandhi, S., Oh, B.-T., Schnoor, J.L. and Alvarez, P.J., 2002. Degradation of TCE, Cr(VI), sulfate, and nitrate mixtures by granular iron in flow-through columns under different microbial conditions. Water Res 36(8), 1973-1982.

Garbisu, C., Alkorta, I., Llama, M.J. and Serra, J.L., 1998. Aerobic chromate reduction by Bacillus subtilis. Biodegradation 9(2), 133-141.

Ge, S., Peng, Y.,Wang, S., Lu, C., Cao, X., Zhu, Y., 2012. Nitrite accumulation under constant temperature in anoxic denitrification process: the effects of carbon sources and COD/NO_3–N. Bioresour. Technol. 114, 137–143

Granger, J., Sigman, D.M., Lehmann, M.F., Tortell, P.D., 2008. Nitrogen and oxygen isotope fractionation during dissimilatory nitrate reduction by denitrifying bacteria. Limnol. Oceanogr. 53, 2533–2545. https://doi.org/10.4319/lo.2008.53.6.2533

Granger, J., and Sigman, D. M. 2009. Removal of nitrite with sulfamic acid for

763 nitrate N and O isotope analysis with the denitrifier method. Rapid
764 Communications in Mass Spectrometry: An International Journal Devoted
765 to the Rapid Dissemination of Up-to-the-Minute Research in Mass
766 Spectrometry, 23(23), 3753-3762.

767 Granger, J., Wankel, S.D., 2016. Isotopic overprinting of nitrification on
768 denitrification as a ubiquitous and unifying feature of environmental
769 nitrogen cycling. Proc. Natl. Acad. Sci. 113, E6391–E6400.
770 https://doi.org/10.1073/pnas.1601383113

771 Grau-Martínez, A., Torrentó, C., Carrey, R., Rodríguez-Escales, P., Domènech,
772 C., Ghiglieri, G., Soler, A., Otero, N., 2017. Feasibility of two low-cost
773 organic substrates for inducing denitrification in artificial recharge ponds:
774 Batch and flow-through experiments. J. Contam. Hydrol. 198, 48–58.
775 https://doi.org/10.1016/j.jconhyd.2017.01.001

776 Grischek, T., Hiscock, K.M., Metschies, T., Dennis, P.F., Nestler, W., 1998.
777 Factors affecting denitrification during infiltration of river water into a sand
778 and gravel aquifer in Saxony, Germany. Water Res. 32, 450–460.

779 Giuliano, M.J., Blarasin, M.T., Panarello, H., 2015. Evaluación de la geoquímica
780 e isótopos del nitrato en el acuífero libre de una llanura con actividad
781 agropecuaria, Córdoba, Argentina. Revista Académica de la Facultad de
782 Ingeniería, Universidad Autónoma de Yucatán, Vol. 19, No.1, ISSN 1665-
783 529-X.

784 Han, R., Qin, L., Brown, S. T., Christensen, J. N., Beller, H. R. 2012. Differential
785 isotopic fractionation during Cr(VI) reduction by an aquifer-derived
786 bacterium under aerobic versus denitrifying conditions. Appl. Environ.

787 Microbiol., 78(7), 2462-2464.

788 Han, R., Geller, J. T., Yang, L., Brodie, E. L., Chakraborty, R., Larsen, J. T.,
789 Beller, H. R., 2010. Physiological and transcriptional studies of Cr(VI)
790 reduction under aerobic and denitrifying conditions by an aquifer-derived
791 pseudomonad. Environmental science and technology, 44(19), 7491-
792 7497.

793 Heikoop, J. M., Johnson, T. M., Birdsell, K. H., Longmire, P., Hickmott, D. D.,
794 Jacobs, E. P., and Vaniman, D. T., 2014. Isotopic evidence for reduction
795 of anthropogenic hexavalent chromium in Los Alamos National
796 Laboratory groundwater. Chemical Geology, 373, 1-9.

797 Ishibashi, Y., Cervantes, C., and Silver, S., 1990. Chromium reduction in
798 Pseudomonas putida. Applied and environmental microbiology, 56(7),
799 2268-2270.

800 Izbicki, J.A., Ball, J.W., Bullen, T.D., Sutley, S.J., 2008. Chromium, chromium
801 isotopes and selected trace elements, western Mojave Desert, USA.
802 Applied Geochemistry, 23(5), 1325-1352.

803 Jamieson-Hanes, J., Gibson, B., Lindsay, M., Kim, Y., Ptacek, C., Blowes, D.,
804 2012a. Chromium isotope fractionation during reduction of Cr (VI) under
805 saturated flow conditions. Environmental Science and Technology, 46,
806 6783-6789.

807 Jamieson-Hanes, J. H., Amos, R. T., Blowes, D. W., 2012b. Reactive transport
808 modeling of chromium isotope fractionation during Cr(VI) reduction.
809 Environmental science & technology, 46(24), 13311-13316.

Johnson, T.M., Bullen, T.D., 2004. Mass-dependent fractionation of seleniumand chromium isotopes in low-temperature environments. In: Johnson, C.M., Beard, B.L., Albarede, F. (Eds.), Geochemistry of non-traditional stable isotopesRev. Mineral. Geochem. 55 (1), 289–317.

Kendall, C., Elliott, E.M., Wankel, S.D., 2007. Tracing anthropogenic inputs of nitrogen to ecosystems. (Chapter 12). In: Michener, R.H., Lajtha, K. (Eds.), Stable Isotopes in Ecology and Environmental Science, second ed. Blackwell Publishing, pp. 375–449

Kim, C., Zhou, Q., Deng, B., Thornton, E.C., Xu, H., 2001. Chromium (VI) Reduction by Hydrogen Sulfide in Aqueous Media: Stoichiometry and Kinetics. Environmental Science & Technology 2001; 35: 2219-2225.

Kitchen, J. W., Johnson, T. M., Bullen, T. D., Zhu, J., and Raddatz, A., 2012. Chromium isotope fractionation factors for reduction of Cr (VI) by aqueous Fe (II) and organic molecules. Geochimica et Cosmochimica Acta, 89, 190-201.

Knöller, K., Vogt, C., Haupt, M., Feisthauer, S., Richnow, H.H., 2011. Experimental investigation of nitrogen and oxygen isotope fractionation in nitrate and nitrite during denitrification. Biogeochemistry 103, 371–384. https://doi.org/10.1007/s10533-010-9483-9

Knowles, R., 1982. Denitrification. Microbiological reviews, 46(1), 43.

Korom, S. F., 1992. Natural denitrification in the saturated zone: a review. Water resources research, 28(6), 1657-1668.

Kotas, J., and Stasicka, Z., 2000. Chromium occurrence in the environment and

833 methods of its speciation. Environ. Pollut, 107, 263–283.

834 Kourtev, P.S., Nakatsu, C.H., Konopka, A., 2009. Inhibition of nitrate reduction
835 by chromium(VI) in anaerobic soil microcosms. Appl. Environ. Microbiol.
836 75, 6249–6257. https://doi.org/10.1128/AEM.00347-09

837 Mancino, C., Vives, L., Funes, A., Zarate, M., Martínez, S., 2013. Modelación
838 del flujo subterráneo en la cuenca Matanza-Riachuelo, provincia de
839 Buenos Aires. 1. Geología y geometría del subsuelo. Temas Actuales de
840 la Hidrología Subterránea. Editorial EDULP, La Plata, pp. 85–92.

841 Margalef-Marti, R., Carrey, R., Viladés, M., Jubany, I., Vilanova, E., Grau, R.,
842 Soler, A., Otero, N., 2019a. Use of nitrogen and oxygen isotopes of
843 dissolved nitrate to trace field-scale induced denitrification efficiency
844 throughout an in-situ groundwater remediation strategy. Science of the
845 Total Environment, 686, 709-718.

846 Margalef-Marti, R., Carrey, R., Soler, A., Otero, N., 2019b. Evaluating the
847 potential use of a dairy industry residue to induce denitrification in
848 polluted water bodies: a flow-through experiment. J. Environ. Manag.,
849 245, 86-94.

850 Mariotti, A., Landreau, A., Simon, B., 1988. 15N isotope biogeochemistry and
851 natural denitrification process in groundwater: application to the chalk
852 aquifer of northern France. Geochim. Cosmochim. Acta 52, 1869–1878.

853 Marsh, T. L., Leon, N. M., & McInerney, M. J., 2000. Physiochemical factors
854 affecting chromate reduction by aquifer materials. Geomicrobiology
855 Journal, 17(4), 291-303.

856 Martínez, D., E., Moschione, E., Bocanegra, M., Glok Galli, R., Aravena. 2014.
857 Distribution and origin of nitrate in groundwater in an urban and suburban
858 aquifer in Mar del Plata, Argentina. Environ Earth Sci.72:1877–1886.

859 Mayer, K.U., Blowes, D.W., Frind, E.O, 2001. Reactive transport modeling of an
860 in situ reactive barrier for the treatment of hexavalent chromium and
861 trichloroethylene in groundwater. Water Resources Research, 37, 3091-
862 3103.

863 McIlvin, M.R., Altabet, M.A., 2005. Chemical conversion of nitrate and nitrite to
864 nitrous oxide for nitrogen and oxygen isotopic analysis in freshwater and
865 seawater. Anal Chem 77, 5589–5595. https://doi.org/10.1021/ac050528s

866 Middleton, S.S., Latmani, R.B., Mackey, M.R., Ellisman, M.H., Tebo, B.M. and
867 Criddle, C.S., 2003. Cometabolism of Cr(VI) by Shewanella oneidensis
868 MR-1 produces cell-associated reduced chromium and inhibits growth.
869 Biotechnol Bioeng 83(6), 627-637.

870 Molokwane, P.E., Chirwa, E.M., 2011. Modelling Cr (VI) removal in a biological
871 permeable reactive barrier: Microcosm simulation. Chemical Engineering
872 Transactions, 24, 1051-1056.

873 Mullet, M., Boursiquot, S., Ehrhardt, J.J. 2004. Removal of hexavalent
874 chromium from solutions by mackinawite, tetragonal FeS. Colloids and
875 Surfaces A: Physicochemical and Engineering Aspects, 244: 77-85.

876 Novak, M., Martinkova, E., Chrastny, V., Stepanova, M., Sebek, O., Andronikov,
877 A., Curik, J., Veselovsky, F., Prechova, E., Houskova, M., Buzek, F.,
878 Farkas, J., Komarek, A., 2017. The fate of Cr(VI) in contaminated

879 aquifers 65 years after the first spillage of plating solutions: A $\delta^{53}Cr$ study
880 at four Central European sites. Catena, 158, 371-380.

881 Otero, N., Torrentó, C., Soler, A., Menció, A., Mas-Pla, J., 2009. Monitoring
882 groundwater nitrate attenuation in a regional system coupling
883 hydrogeology with multi-isotopic methods: the case of Plana de Vic
884 (Osona, Spain). Agric. Ecosyst. Environ. 133, 103–113.

885 Palmer, C.D., and Wittbrodt, P.R., 1991. Processes affecting the remediation of
886 chromium contaminated sites. Environ. Health Perspectives, 92, 25–40.

887 Panagiotakis, I., Dermatas, D., Vatseris, C., Chrysochoou, M., Papassiopi, N.,
888 Xenidis, A., Vaxevanidou, K., 2015. Forensic investigation of a chromium
889 (VI) groundwater plume in Thiva, Greece. Journal of hazardous
890 materials, 281, 27-34.

891 Panno, S. V., Hackley, K. C., Hwang, H. H., & Kelly, W. R., 2001. Determination
892 of the sources of nitrate contamination in karst springs using isotopic and
893 chemical indicators. Chemical Geology, 179(1-4), 113-128.

894 Pauwels, H., Foucher, J. C., & Kloppmann, W., 2000. Denitrification and mixing
895 in a schist aquifer: influence on water chemistry and isotopes. Chemical
896 Geology, 168(3-4), 307-324.

897 Pettine, M., D'Ottone, L., Campanella, L., Millero, F.J., Passino, R., 1998b. The
898 reduction of chromium (VI) by iron (II) in aqueous solutions. Geochimica
899 et Cosmochimica Acta, 62: 1509-1519.

900 Puig, R., Soler, A., Widory, D., Mas-Pla, J., Domènech, C., and Otero, N., 2017.
901 Characterizing sources and natural attenuation of nitrate contamination in

902 the Baix Ter aquifer system (NE Spain) using a multi-isotope approach.
903 Science of the Total Environment, 580, 518-532.

904 Raddatz, A.L., Johnson, T.M., McLing, T.L., 2011. Cr stable isotopes in Snake
905 River Plain aquifer groundwater: evidence for natural reduction of
906 dissolved Cr(VI). Environ. Sci. Technol. 45 (2), 502–507.

907 Rai, D., Eary, L.E., Zachara, J.M., 1989. Environmental chemistry of chromium.
908 Science of The Total Environment, 86, 15–23.

909 Rivett, M. O., Buss, S. R., Morgan, P., Smith, J. W. N. & Bemment, C. D. Nitrate
910 attenuation in groundwater: A review of biogeochemical controlling
911 processes. *Water Res.* **42,** 4215–4232 (2008).

912 Richard, F.C., Bourg, A.C.M., 1991. Aqueous geochemistry of chromium: A
913 review. Water Research, 25: 807-816.

914 Ryabenko, E., Altabet, M. a., Wallace, D.W.R., 2009. Effect of chloride on the
915 chemical conversion of nitrate to nitrous oxide for $\delta^{15}N$ analysis. Limnol.
916 Oceanogr. Methods 7, 545–552. https://doi.org/10.4319/lom.2009.7.545

917 Salvador, C., 2013. Historia de la Industria Curtidora Argentina. Ed. Dunken
918 320p.

919 Schoenberg, R., Zink, S., Staubwasser, M., von Blanckenburg, F., 2008. The
920 stable Cr isotope inventory of solid Earth reservoirs determined by
921 double spike MC-ICP-MS. Chem. Geol. 249 (3–4), 294–306.

922 Schauble, E., Rossman, G., Taylor, Jr.H., 2004. Theoretical estimates of
923 equilibrium chromium-isotope fractionations. Chemical Geology, 205, 99-
924 114.

925 Schlautman, M.A., and Han, I., 2001. Effects of pH and dissolved oxygen on the
926 reduction of hexavalent chromium by dissolved ferrous iron in poorly
927 buffered aqueous systems. Water Research, 35: 1534-1546.

928 Scott, K., Lu, X., Cavanaugh, C., Liu, J., 2004. Optimal methods for estimating
929 kinetic isotope effects from different forms of the Rayleigh distillation
930 equation. Geochimica et Cosmochimica Acta, 68, 433-442.

931 Sigman, D.M., Casciotti, K.L., Andreani, M., Barford, C., Galanter, M., Böhlke,
932 J.K., 2001. A bacterial method for the nitrogen isotopic analysis of nitrate
933 in seawater and freshwater. Anal. Chem. 73, 4145–4153.

934 Sikora, E. R., Johnson, T. M., and Bullen, T. D., 2008. Microbial mass-
935 dependent fractionation of chromium isotopes. Geochimica et
936 Cosmochimica Acta, 72(15), 3631-3641.

937 Torrentó, C., Urmeneta, J., Otero, N., Soler, A., Viñas, M., Cama, J., 2011.
938 Enhanced denitrification in groundwater and sediments from a nitrate
939 contaminated aquifer after addition of pyrite. Chem. Geol. 287, 90–101.

940 Trinquier, A., Elliott, T., Ulfbeck, D., Coath, C., Krot, A.N., Bizzarro,M., 2009.
941 Origin of nucleosynthetic isotope heterogeneity in the solar
942 protoplanetary disk. Science 324, 374–376.
943 http://dx.doi.org/10.1126/science.1168221

944 Tsushima, I., Ogasawara, Y., Kindaichi, T., Satoh, H., Okabe, S., 2007.
945 Development of high-rate anaerobic ammonium-oxidizing (anammox)
946 biofilm reactors. Water research, 41(8), 1623-1634.

947 Vatsouria, A., Vainshtein, M., Kuschk, P., Wiessner, A., Kosolapov, D. and

948 Kaestner, M., 2005. Anaerobic co-reduction of chromate and nitrate by
949 bacterial cultures of Staphylococcus epidermidis L-02. Journal of
950 Industrial Microbiology and Biotechnology 32(9), 409-414.

951 Viamajala, S., Peyton, B.M., Apel, W.A. and Petersen, J.N., 2002.
952 Chromate/nitrite interactions in Shewanella oneidensis MR-695 1:
953 Evidence for multiple hexavalent chromium [Cr(VI)] reduction
954 mechanisms dependent on physiological growth conditions. Biotechnol
955 Bioeng 78(7), 770-778.

956 Vidal-Gavilan, G., Folch, A., Otero, N., Solanas, A.M., Soler, A., 2013. Isotope
957 characterization of an in situ biodenitrification pilot-test in a fractured
958 aquifer. Applied Geochemistry, 32, 153–163.

959 Vives, L., Scioli, C., Mancino, C., Martínez, S., 2013. Modelación del flujo
960 subterráneo en la cuenca Matanza Riachuelo, Provincia de Buenos
961 Aires. 3. Modelo numérico de flujo. In: González, N., Kruse, E., Trovatto,
962 M., Laurencena, P. (Eds.), Temas actuales de la hidrología subterránea.
963 Editorial EDULP, La Plata, pp. 101–108.

964 Wanner, C., Eggenberger, U., Kurz, D., Zink, S., and Mäder, U. 2012a. A
965 chromate-contaminated site in southern Switzerland–Part 1: Site
966 characterization and the use of Cr isotopes to delineate fate and
967 transport. Applied geochemistry, 27(3), 644-654.

968 Wanner, C., Eggenberger, U., and Mäder, U. 2012b. A chromate-contaminated
969 site in southern Switzerland–Part 2: Reactive transport modeling to
970 optimize remediation options. Applied geochemistry, 27(3), 655-662.

971 Wanner, C., Zink, S., Eggenberger, U., Mäder, U., 2012c. Assessing the Cr (VI)
972 reduction efficiency of a permeable reactive barrier using Cr isotope
973 measurements and 2D reactive transport modeling. Journal of
974 Contaminant Hydrology, 131, 54-63.

975 Wilkin, R. T., Su, C., Ford, R. G., Paul, C. J. 2005. Chromium-removal
976 processes during groundwater remediation by a zerovalent iron
977 permeable reactive barrier. Environmental science & technology, 39(12),
978 4599-4605.

979 Wunderlich, A., Meckenstock, R., Einsiedl, F., 2012. Effect of different carbon
980 substrates on nitrate stable isotope fractionation during microbial
981 denitrification. Environ. Sci. Technol. 46, 4861–4868.
982 https://doi.org/10.1021/es204075b

983 Wunderlich, A., Meckenstock, R.U., Einsiedl, F., 2013. A mixture of nitrite-
984 oxidizing and denitrifying microorganisms affects the $\delta^{18}O$ of dissolved
985 nitrate during anaerobic microbial denitrification depending on the $\delta^{18}O$ of
986 ambient water. Geochim. Cosmochim. Acta 119, 31–45.
987 https://doi.org/10.1016/j.gca.2013.05.028

988 Zabala, M.E., Manzano, M., Vives, L., 2016. Groundwater chemical baseline
989 values to assess the Recovery Plan in the Matanza-Riachuelo River
990 basin Argentina. Science of the Total Environment, 541 1516-1530.

991 Zink, S., Schoenberg, R., Staubwasser, M., 2010. Isotopic fractionation and
992 reaction kinetics between Cr(III) and Cr(VI) in aqueous media.
993 Geochimica et Cosmochimica Acta, 74, 5729-5745.

994

995 **TABLES AND FIGURES**

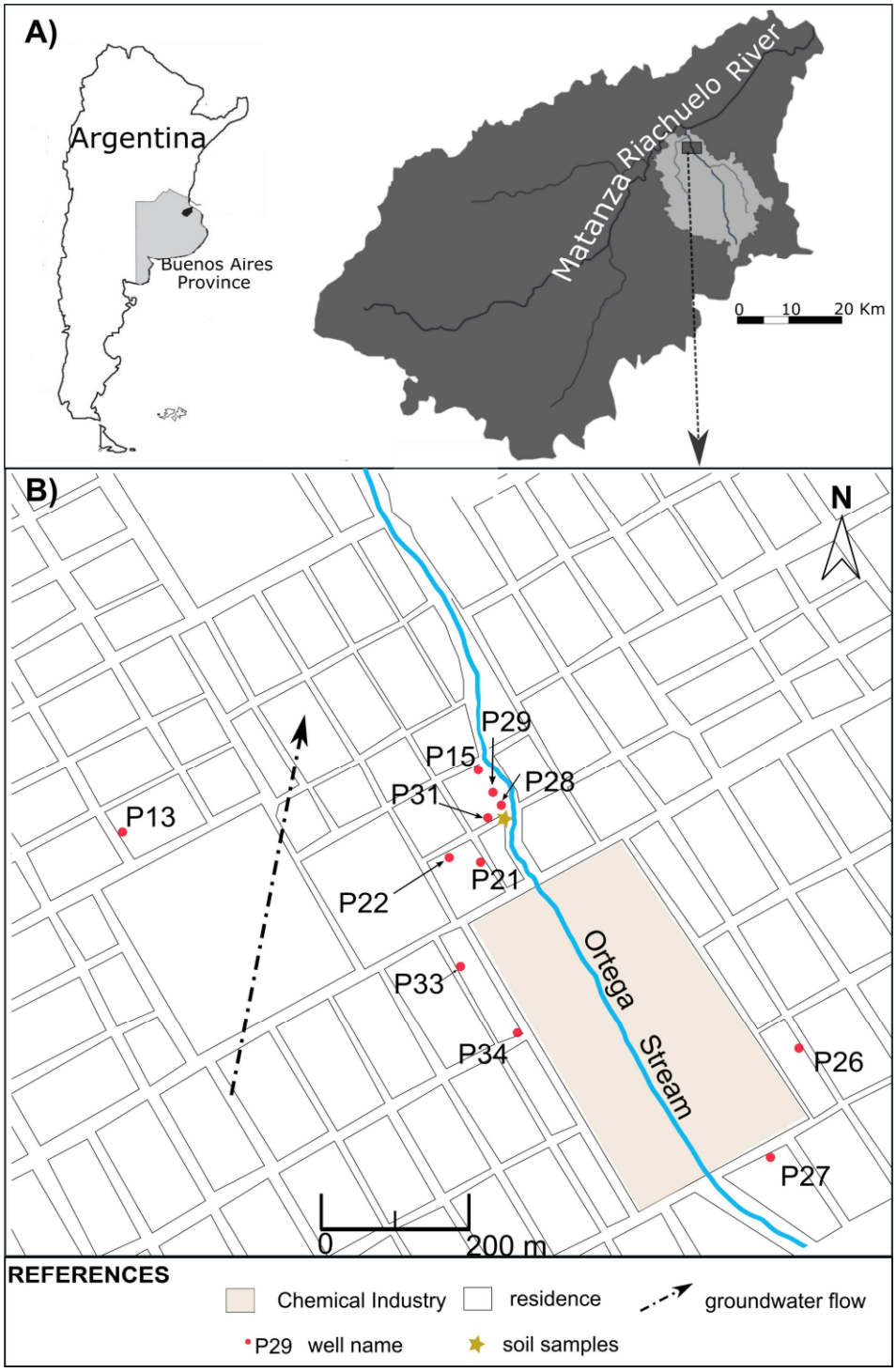

996

997 **Figure 1:** A) Location of the Matanza-Riachuelo River Basin (MRB), and Ortega stream sub

998 basin. B) Site of study, San Ignacio neighbourhood.

999

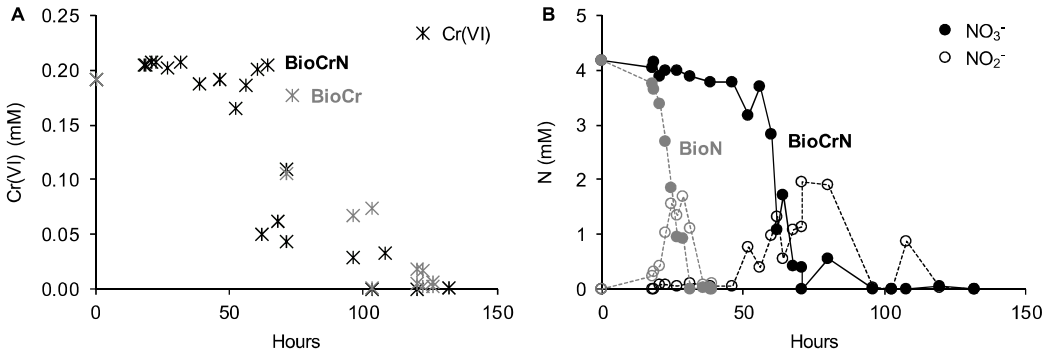

1000

1001 **Figure 2. Cr(VI) and NO_3^- concentration evolution during the laboratory experiments. A)**

1002 Cr(VI) reduction by ethanol in the presence (black) and absence (grey) of NO_3^- and **B)** NO_3^-

1003 reduction by ethanol in the presence (black) and absence (grey) of Cr(VI).

1004

1005

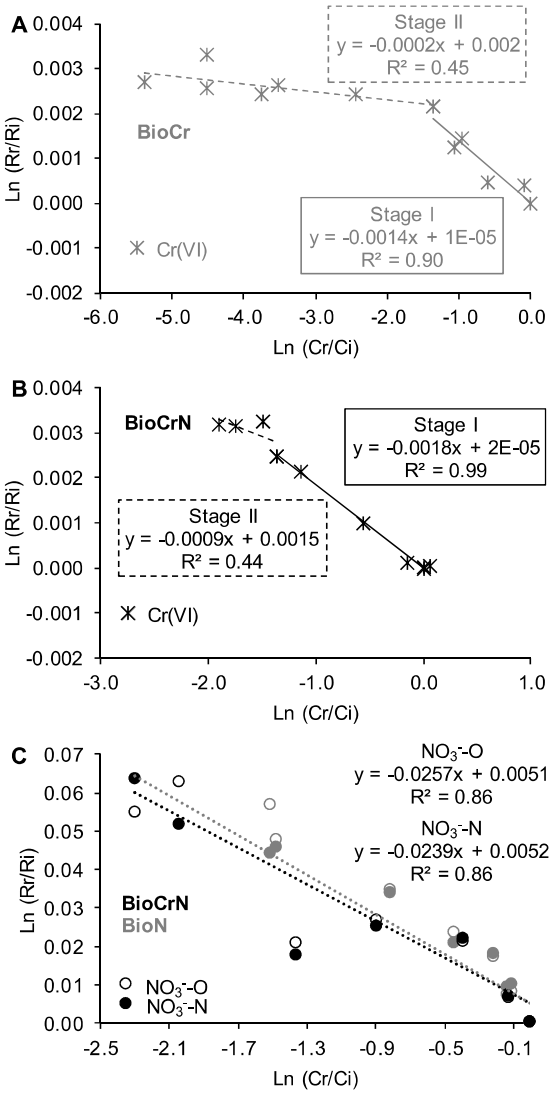

1006

1007 **Figure 3. Cr(VI) and NO_3^- isotopic fractionation during the batch experiments. A)** $\varepsilon^{53}Cr$

1008 calculated for the BioCr experiments, **B)** $\varepsilon^{53}Cr$ calculated for the BioCrN experiments and **C)**

1009 $\varepsilon^{15}N_{NO3}$ (full circles) and $\varepsilon^{18}O_{NO3}$ (empty circles) calculated for the BioN (grey) and BioCrN

1010 (black) experiments.

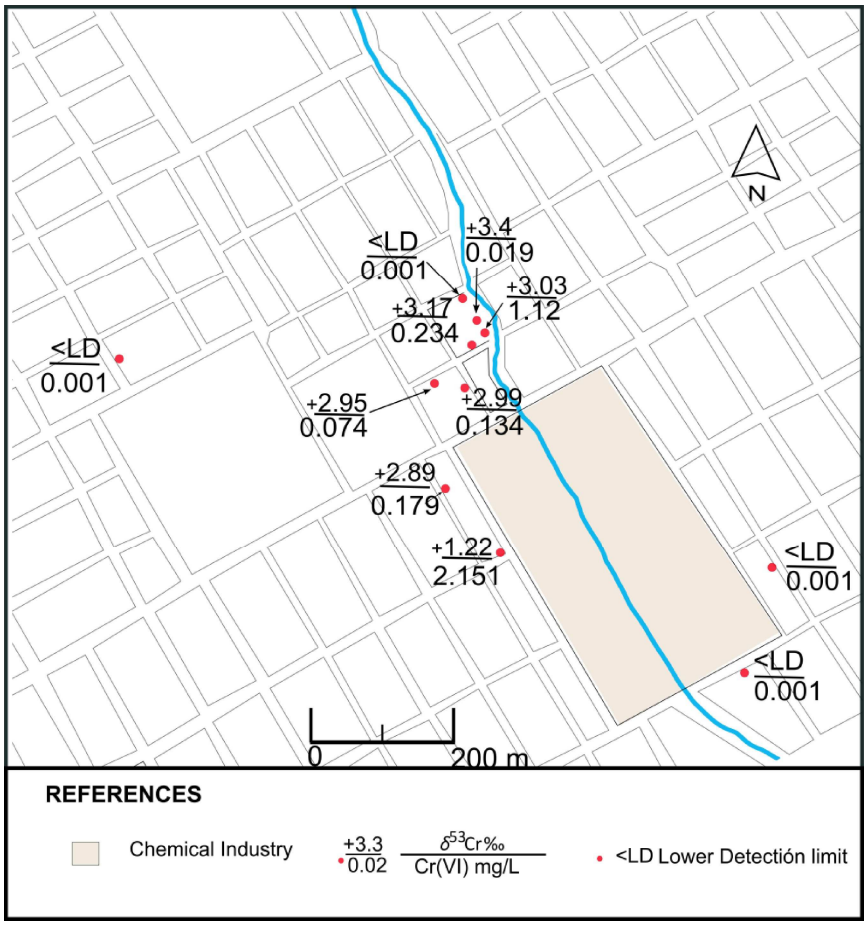

1011

1012 **Figure 4:** Spatial distribution of δ^{53}Cr and Cr(VI) in San Ignacio neighbourhood.

1013

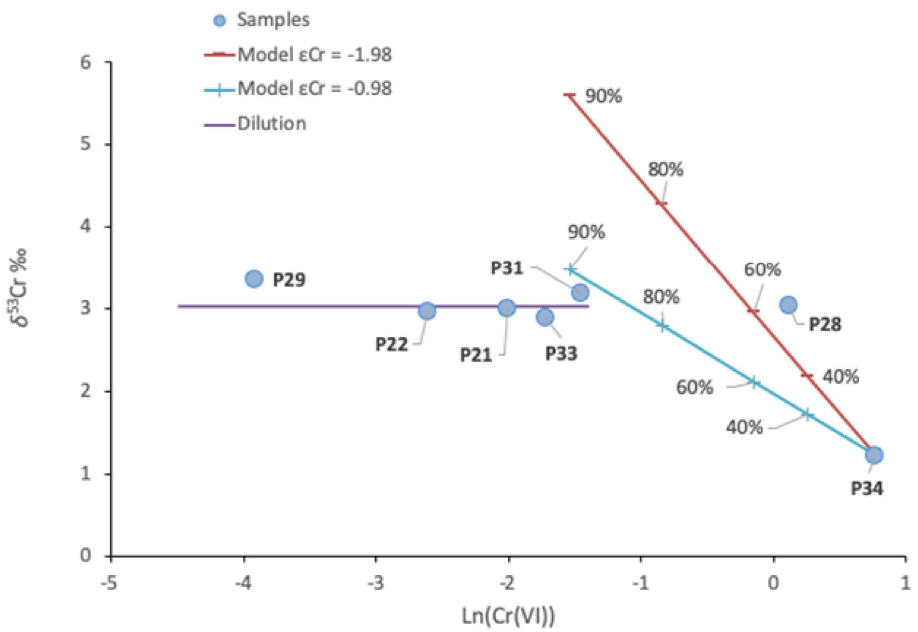

Figure 5: Values of ε^{53}Cr vs. Ln Cr(VI). The red line represents a Rayleigh model calculated with stage I ε^{53}Cr and the blue line represents a Rayleigh model calculated with stage II ε^{53}Cr, obtained from BioCrN experiment. The purple line represents dilution with unpolluted groundwater.

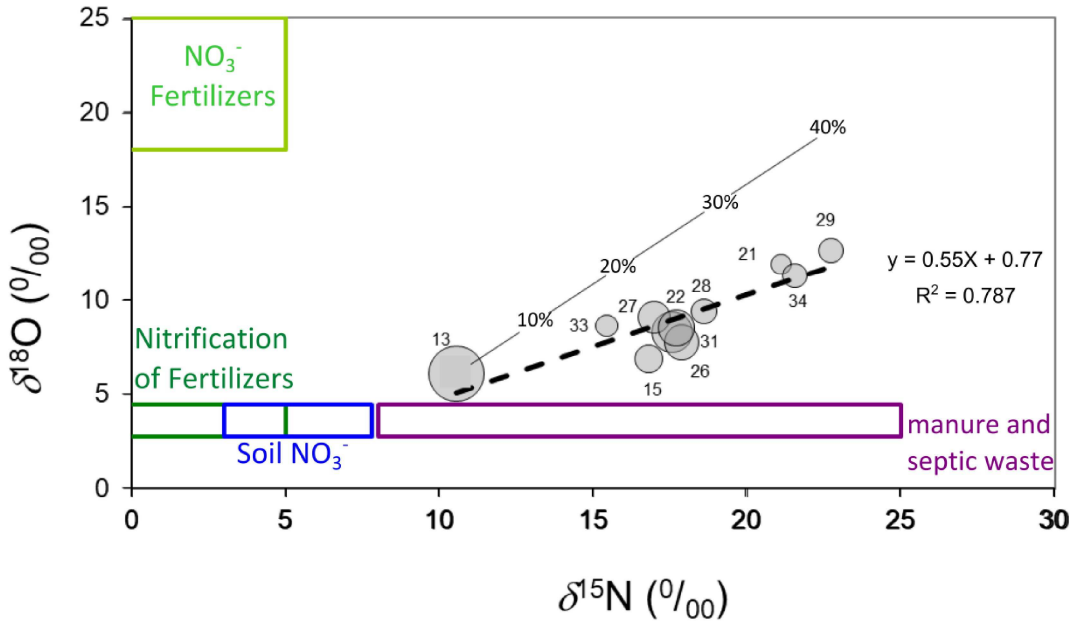

Figure 6: Estimated percentage of denitrification in the study site, quantified by using the Rayleigh equation and the ε values obtained in the BioCrN experiments. The boxes of the nitrate sources are from Vitòria et al (2004, and references therein). The solid line represents the model used to calculate the denitrification percentage, and the dotted line is the linear regression of the field samples.

Table 1. Series of laboratory experiments. Tested conditions and microcosms composition. Cr(VI) was added as $K_2Cr_2O_7$ salt and NPDOC as ethanol, NO_3^- was already present in groundwater. The blank microcosms contained only sediment and deionized water (DIW).

Series	Condition	Replicates	NO_3^- (mM)	Cr(VI) (mM)	NPDOC (mM)
BioCr	Biostimulated	12	0	0.2	8.4
BioN	Biostimulated	12	4.2	0	11.8
BioCrN	Biostimulated	23	4.2	0.2	11.8
CtrlCrN	Control	3	4.2	0.2	0
Blank	DIW	3	0	0	0

1036 **Table 2. Standards used for the isotopic analysis.** According to Coplen (2011), several
1037 international and laboratory (CCiT) standards were interspersed among samples for the
1038 normalisation of the results.

Analysis	International standards	Laboratory standards
$\delta^{53}Cr$	NIST SRM 979 and NIST 3112a	
$\delta^{15}N_{NO3}$	USGS-32, USGS-34, USGS-35	CCiT-IWS ($\delta^{15}N$ = +16.9 ‰)
$\delta^{18}O_{NO3}$	USGS-32, USGS-34, USGS-35	CCiT-IWS ($\delta^{18}O$ = +28.5 ‰).

1039
1040

1041

1042 **Table 3:** Chemical and isotopic data of the samples extracted in the batch experiments (n.d. =

1043 not determined, <LD = below the detection limit).

Experiment	Time (Hours)	NPDOC (mM)	Cr(VI) (mM)	NH_4^+ (mM)	NO_2^- (mM)	NO_3^- (mM)	$\delta^{53}Cr$ (‰)	$\delta^{15}N$-NO_3^- (‰)	$\delta^{18}O$-NO_3^- (‰)
BioCr	0	8.4	0.19	n.d	n.d.	n.d.	n.d	n.d.	n.d.
	71	24.5	0.106	n.d.	n.d.	n.d.	+0.5	n.d.	n.d.
	73	7.9	0.177	n.d.	n.d.	n.d.	+0.4	n.d.	n.d.
	96	21.1	0.067	n.d.	n.d.	n.d.	+1.3	n.d.	n.d.
	103	20.7	0.001	n.d.	n.d.	n.d.	+2.8	n.d.	n.d.
	103	20.1	0.058	n.d.	n.d.	n.d.	+1.5	n.d.	n.d.
	120	17.2	0.018	n.d.	n.d.	n.d.	n.d.	n.d.	n.d.
	120	14.1	0.004	n.d.	n.d.	n.d.	+2.5	n.d.	n.d.
	122	13.0	0.003	n.d.	n.d.	n.d.	+3.4	n.d.	n.d.
	122	12.6	0.014	n.d.	n.d.	n.d.	+2.5	n.d.	n.d.
	126	18.6	0.003	n.d.	n.d.	n.d.	+2.7	n.d.	n.d.
	126	21.4	0.003	n.d.	n.d.	n.d.	+2.6	n.d.	n.d.
BioN	0	11.8	n.d.	<LD	<LD	4.2	n.d.	+11.2	+7.1
	18	9.0	n.d.	<LD	0.2	3.8	n.d.	+21.3	+15.1
	18.5	8.9	n.d.	<LD	0.3	3.7	n.d.	+20.6	+14.2
	20.5	9.1	n.d.	<LD	0.4	3.4	n.d.	+29.4	+24.5
	22.5	8.5	n.d.	<LD	1	2.7	n.d.	+32.2	+30.8
	24.5	7.5	n.d.	<LD	1.6	1.9	n.d.	+46.0	+42.4
	26.5	6.9	n.d.	<LD	1.4	1	n.d.	+58.3	+56.3
	28.5	7.2	n.d.	<LD	1.7	0.9	n.d.	+56.5	+65.7
	31.5	5.8	n.d.	<LD	1.1	<LD	n.d.	n.d.	n.d.
	36	4.0	n.d.	<LD	0.1	<LD	n.d.	n.d.	n.d.

	38.5	6.8	n.d.	<LD	0	<LD	n.d.	n.d.	n.d.
	39	3.4	n.d.	<LD	0.1	<LD	n.d.	n.d.	n.d.
	0	11.8	0.192	<LD	<LD	4.2	n.d.	+11.2	+7.1
	18	8.9	0.205	<LD	<LD	4.1	n.d.	n.d.	n.d.
	18.5	9.8	0.2	<LD	<LD	4.2	+0.1	n.d.	n.d.
	20.5	8.8	0.208	<LD	0.1	3.9	n.d.	n.d.	n.d.
	22.5	8.9	0.209	<LD	0.1	4	n.d.	9.9	6.9
	26.5	9.3	0.203	<LD	<LD	4	n.d.	n.d.	n.d.
	31.5	9.3	0.2	<LD	0.1	3.9	n.d.	n.d.	n.d.
	38.5	9.2	0.188	<LD	0.05	3.8	n.d.	n.d.	n.d.
	46	8.5	0.192	<LD	0.1	3.8	+0.1	n.d.	n.d.
	52	5.4	0.165	<LD	0.8	3.2	+0.2	n.d.	n.d.
	56	6.3	0.190	<LD	0.4	3.7	n.d.	+18.2	+13.7
BioCrN	60	7.2	0.200	<LD	1	2.8	n.d.	+33.6	+28.5
	62	6.6	0.049	<LD	1.3	1.1	+2.6	+29.0	+28.1
	64	5.8	0.2	<LD	0.6	1.7	n.d.	+36.7	+34.2
	68	5.2	0.061	<LD	1.1	0.4	+2.2	+77.4	+63.7
	71	5.7	0.043	<LD	1.1	0.4	+3.3	n.d.	n.d.
	71	7.1	0.110	<LD	2	0	+1.1	n.d.	n.d.
	80	7.5	n.d.	<LD	1.9	0.5	n.d.	+64.8	+72.2
	96	5.6	0.029	<LD	<LD	0	+3.3	n.d.	n.d.
	103	0	0.002	<LD	<LD	0	n.d.	n.d.	n.d.
	108	6.8	0	<LD	0.9	0	+3.2	n.d.	n.d.
	120	6.8	0.033	<LD	0	0	n.d.	n.d.	n.d.
	132	6.5	0.0004	<LD	0	0	n.d.	n.d.	n.d.

1044

1045 **Table 3:** Chemical and isotopic data of the samples extracted in the batch experiments (cont.)

	Time	NPDOC	Cr(VI)	NH_4^+	NO_2^-	NO_3^-	$\delta^{53}Cr$	$\delta^{15}N$-NO_3^-	$\delta^{18}O$-NO_3^-
	(Hours)	(mM)	(mM)	(mM)	(mM)	(mM)	(‰)	(‰)	(‰)
CtrlCrN-0	38.5	n.d.	n.d.	n.d.	0	4.2	n.d.	n.d.	n.d.
CtrlCrN-1	71	0.3	0.2	0	0	4.6	0	n.d.	n.d.
CtrlCrN-2	263	0.3	n.d.	0	0	4.5	n.d.	n.d.	n.d.
Blank-0	38.5	0.9	n.d.	0	0	0	n.d.	n.d.	n.d.
Blank-1	38.5	0.5	n.d.	0	0	0	n.d.	n.d.	n.d.
Blank-2	71	n.d.	n.d.	0	0	0	n.d.	n.d.	n.d.

1046

1047

1048 **Table 4:** Chemical and isotopic data from groundwater samples taken from the San Ignacio neighbourhood.

sample	Well depth	Aquifer	pH	OD	EC	DOC	Ca^{2+}	Mg^{2+}	K^{+}	Na^{+}	NH_4^{+}	SO_4^{2-}	Cl^{-}	NO_2^{-}	NO_3^{-}	Cr(VI)	$\delta^{53}Cr$	$\delta^{15}N$-NO_3^{-}	$\delta^{18}O$-NO_3^{-}
Nº	(m)			(mM)	(µm s/cm)	(mM)	(mM)	(mM)	(mM)	(mM)	(mM)	(mM)	(mM)	(mM)	(mM)	(mM)	(‰)	(‰)	(‰)
P13	20	Upper	7.1	0.14	1386	0.08	1.0	1.3	0.4	9.5	0.002	0.4	3.1	<0.002	3.9	1.9E-05	<LD	+10.6	+6.1
P14	15	Upper	7.9	NM	2000	0.14	1.1	2.1	0.6	15.7	0.001	0.9	6.5	<0.002	1	1.9E-05	<LD	+16.8	+6.9
P21	15	Upper	7.9	NM	1727	0.14	1.0	1.7	0.4	12	0.003	1.1	5	<0.002	0.5	0.003	+2.9	+21.1	+11.9
P22	15	Upper	8.0	NM	1085	0.17	0.8	1.3	0.4	13	0.002	0.9	3.5	<0.002	2.1	0.001	+2.9	+17.6	+8.3
P26	15	Upper	8.1	NM	1755	0.08	1.0	1.5	0.5	13.2	0.002	0.4	2.8	<0.002	1.5	1.9E-05	<LD	+17.9	+7.9
P27	15	Upper	8.0	NM	992	0.12	1.1	1.3	0.4	5.2	0.013	0.4	2.6	<0.002	1.3	1.9E-05	<LD	+17	+9.1
P28	40	Puelche	7.3	0.22	1803	0.07	0.5	0.6	0.2	6.2	0.004	0.9	5.3	<0.002	0.8	0.022	+3	+18.6	+9.4
P29	15	Upper	6.9	0.02	1696	0.20	1.1	0.9	0.3	4.7	0.004	0.3	1.6	<0.002	0.8	0.0004	+3.4	+22.8	+12.7
P31	15	Upper	NM	NM	NM	0.08	1.0	0.9	0.3	8.7	0.004	0.9	4.2	<0.002	1.7	0.005	+3.2	+17.7	+8.5
P33	15	Upper	7.9	NM	2060	0.07	2.7	2.5	0.4	11.3	0.004	4.4	1.7	<0.002	0.6	0.003	+2.9	+15.5	+8.7
P34	15	Upper	NM	NM	1424	0.12	1.1	1.1	0.3	8.7	0.004	0.2	1.8	<0.002	0.8	0.041	+1.2	+21.6	+11.4

1049

1050

1051 **Table 5. Calculated ε for the tested conditions at the laboratory.** ε values obtained for the

1052 Cr(VI) and NO_3^- reduction by ethanol under different conditions.

Series	Composition	$\varepsilon^{53}Cr$ (‰)	$\varepsilon^{15}N_{NO3}$ (‰)	$\varepsilon^{18}O_{NO3}$ (‰)	$\varepsilon^{15}N/\varepsilon^{18}O$
BioCr	Groundwater + sediment + Cr(VI) + ethanol	-1.4 (stage I) -0.2 (stage II)	n.d.	n.d.	n.d.
BioN	Groundwater (NO_3^-) + sediment+ ethanol	n.d.	-23.9	-25.7	0.9
BioCrN	Groundwater (NO_3^-) + sediment+ Cr(VI) + ethanol	-1.8 (stage I) -0.9 (stage II)	-23.9	-25.7	0.9

1053

1054